Mecatronics-2014-Tokyo
November 27-29, 2014, Tokyo, Japan

Robot Navigation in Dynamic Environment using Navigation function APF with SLAM

Soh Iizuka
Dept. of Robots and Mechatronics
Tokyo Denki University
Tokyo, Japan
Email: iizukas@mail.suzulab.fr.dendai.ac.jp
Telephone: +81-03-5284-5151
Fax: +81-03-5284-5151

Takahiko Nakamura
Dept. of Robots and Mechatronics
Tokyo Denki University
Tokyo, Japan
Email: nakamurat@mail.suzulab.fr.dendai.ac.jp
Telephone: +81-03-5284-5151
Fax: +81-03-5284-5151

Satoshi Suzuki
Dept. of Robots and Mechatronics
Tokyo Denki University
Tokyo, Japan
Email: ssuzuki@fr.dendai.ac.jp
Telephone: +81-03-5284-5151
Fax: +81-03-5284-5151

***Abstract*—This paper proposes a technique for navigation of a watch over robot in a dynamic environment. In order to make an environmental map around the robot, the localization of robot and the orbit generation to move avoiding the moving obstacles are required in a dynamics environment. In this study the localization of robot and the environmental map are obtained by using Simultaneous Localization and Mapping (SLAM) which makes the map by using LRF with characteristic markers. The orbit generation to avoid the moving obstacles is executed by using Navigation function that is a type of Artificial Potential Field (APF) method. The generation of an environmental map was simulated by using SLAM on the topology space. It was verified whether a robot using APF was possible to move avoiding the moving obstacles in a dynamic environment through the simulation.**

I. Introduction

Recently, the number of parents who work caring for children by utilizing kindergarten has been increasing in Japan. Due to this circumstance, childminders have more work [1]. Therefore, for instance, a system which simplifies making reports about child's activity in the kindergaten has been developed by utilizing a smart phone as a communication tool [2] [3]. There is, however, a problem that the childminder cannot keep watching over children anytime, and the data entry works are also troublesome for them. Therefore, a concept of Kinder Garden System was proposed from authors' research group [4]. To know the social behavior, environmental factors in their living space have to be investigated because our human activity changes according to the place and equipments in the living space. For this aim, techniques to build a map of the kindergarten and to measure the position of children are required. Further, an automatic updating to built a map is desired because the layout in the kindergarten room changes according to their growth status and personal organization. For this task, a mobile robot with Simultaneous Localization And Mapping (SLAM) is suitable. The map is updated detecting the person from a dynamic object after the map is made.

On the other hand,as a traditional technique of the robot navigation in a dynamic environment, the static obstacle avoidance method [5] and the method forecasting the moving objects [6] are known. The former does not cope with the moving objects, the latter type does not used in general environment because the observation for a long time is needed. Therefore, The orbit generation method by which the robot avoids the obstacle uses Artificial Potential Function (APF) [7]. APF is effective in a dynamic environment because the amount of calculation is small: hence this method is adequate for the real-time computation.

It is verified whether a robot using APF was possible to move avoiding the moving obstacles in a dynamic environment. The remain of this paper is organized as follows: Section II explains the algorithm of SLAM with comb-shaped markers. Section III explains the algorithm of APF which adjusts to a dynamic environment. Section IV verifies the algorithm through simulation, and confirms whether it is possible for a virtual robot to move without collision to other moving objects using APF. Section V describes the conclusion.

II. SLAM algorithm

A. Robot operation model

In our previous study, a basic algorithm to compute position of landmark (LM) named conb-shaped marker was presented [8]. Even if the layout in the kindergarten is changed, comb-shaped marker can be simply set to the wall.

A two-wheel differential mobile robot is assumed for this study. The state of the robot is defined as $\mathbf{x}_t := [x, y, \theta]_t^T \in \mathscr{R}^3$, where, x and y represent coordinate value of the robot, and θ represents attitude angle. Subscript t represents the sampling time index, and same notation is used below. An input vector $\mathbf{u}$ is defined as $\mathbf{u} := [v, \omega]^T$, where $\mathbf{u}$ is a translational velocity, and ω is an angular velocity. Then, the robot kinematics model is expressed as

$$\mathbf{x}_{t+1} = \mathbf{x}_t + \mathbf{g}(\mathbf{x}_t, \mathbf{u}_t), \tag{1}$$

where $\mathbf{g}$ is computed as follows.

$$\mathbf{g} = \begin{cases} \begin{bmatrix} -\frac{v}{\omega}\sin\theta + \frac{v}{\omega}\sin(\theta + \omega\cdot\Delta) \\ \frac{v}{\omega}\cos\theta + \frac{v}{\omega}\cos(\theta + \omega\cdot\Delta) \\ \omega\cdot\Delta \end{bmatrix}_t & (\omega \neq 0) \quad (2) \\ \begin{bmatrix} v\cos\theta\cdot\Delta \\ v\sin\theta\cdot\Delta \\ 0 \end{bmatrix}_t & (\omega = 0) \quad (3) \end{cases}$$

For latter calculations, the Jacobian of the kinematic model concerning $\mathbf{x}$ and $\mathbf{u}$ are denoted as $\mathbf{G} = \frac{\partial \mathbf{g}(\mathbf{x},\mathbf{u})}{\partial \mathbf{x}}$ and $\mathbf{V} = \frac{\partial \mathbf{g}(\mathbf{x},\mathbf{u})}{\partial \mathbf{u}}$, respectively.

B. Derivation of the sensor model

Comb-shaped markers are measured by laser range finder (LRF) and extracted as LM. The distance and orientation from reference point of the robot to LM is calculated by using the data of LRF. Therefore, the sensor model is constructed. Hereafter, The left superscript j is used by a vector element distinguished from another as j th of LM. $\mathbf{m} := [m_x, m_y]^T$ is defined as the position vector of LM, where m_x and m_y are coordinate values of LM. Sensor measurement model ${}^{(j)}h(\mathbf{x},\mathbf{m})$ in case of LRF is given as follows.

$$ {}^{(j)}h(\mathbf{x},\mathbf{m}) := \begin{bmatrix} \sqrt{({}^{(j)}m_x - x)^2 + ({}^{(j)}m_y - y)^2} \\ \mathrm{atan2}({}^{(j)}m_y - y, {}^{(j)}m_x - x) - \theta \end{bmatrix}. \quad (4) $$

Jacobian ${}^{(j)}H_t$ of jth LM for ${}^{(j)}h(\mathbf{x},\mathbf{m})$ concerning $\mathbf{x}(= [x, y, \theta]^T)$ is calculated by $\frac{\partial {}^{(j)}h(\mathbf{x},\mathbf{m})}{\partial \mathbf{x}} =: {}^{(j)}H_t$.

C. Position estimation algorithm using EKF-SLAM

Summarizing the elements of $\mathbf{m}$ and other one $\mathbf{x}$, an augmented state vector $\mathbf{y}$ is defined as

$$ \mathbf{y} = \left[x, y, \theta, {}^{(i)}m_x, {}^{(i)}m_y, \ldots, {}^{(N)}m_x, {}^{(N)}m_y\right]^T \in R^{3N+3}, \quad (5) $$

where N is the number of LM and N is assumed to be already known. Then, the augmented state $\mathbf{y}$ is estimated using $\mathbf{g}(\mathbf{x},\mathbf{u})$.

$$ \mathbf{y}_{t+1} = \mathbf{y}_t + F^T \cdot \mathbf{g}(\mathbf{p}_t, \mathbf{u}_t), \quad (6) $$

where $\mathbf{F}$ is a coefficient matrix to extract the component corresponding to $\mathbf{x}$ from $\mathbf{y}$. In addition, Jacobian G concerning $\mathbf{y}$ is computed by

$$ \mathbf{G}_t = \mathbf{I}_{(3+3N)} + \mathbf{F}^T \mathbf{G} \mathbf{F}. \quad (7) $$

In our SLAM, Extended Kalman Filter-SLAM (EKF-SLAM) is utilized. EKF-SLAM is an algorithm to compute the belief for $\mathbf{y}$ at time t by using estimated average μ_t and covariance Σ_t for $\mathbf{y}$. EKF-SLAM consists of two steps: the prediction step and the correction step. Specifically, an estimated average $(\bar{\mu}_t)$ of next step is computed by using a model from previous estimated value μ_{t-1} ⟨Prediction step⟩. Then, the amount of the forecast measurement $\hat{z}_t$ is calculated by the next expression.

$$ {}^{(i)}\hat{z}_t = [\sqrt{q'}, \mathrm{atan2}(\delta'_y, \delta'_x) - \bar{\theta}_t]^T, \quad (8) $$

where $q' := \delta'^2_x + \delta'^2_y$, $\delta'_x := {}^{(j)}\bar{m}_x - \bar{x}_t$, $\delta'_y := {}^{(j)}\bar{m}_y - \bar{y}_t$. $\bar{x}$ and $\bar{y}$ are extracted as $\bar{x} \leftarrow \mu_{t-1} \mid \mathbf{x}$, and $\bar{y} \leftarrow \mu_{t-1} \mid \mathbf{y}$. And, the error $(z_t - \hat{z}_t)$ between the measured value z_t and $\hat{z}_t$ is obtained, where z is an actual measured value. Depending on covariance matrix Σ_t, the estimated average $\bar{\mu}_t$ is updated according to the prediction difference ⟨Correction step⟩. Refer [8] for the details of the algorithm.

III. Topology space to generated path

Rough path generation is required for the SLAM robot to move inside an environment that will be searched by the robot even if the SLAM technique is used. During the explorer with SLAM, it is necessary to avoid obstacles, and APF-based navigation methods is suitable because of its simplicity and high real-time performance.

In our study, navigation function was used for path finding. Navigation function treats both the work space and the obstacles as topological elements, and it is easy to be expanded to the dynamic environment navigation. For the computation using Navigation function, a diffeomorphic mapping is needed to map the shape of a real space to a topological space. In our study, to simplify it for easy implementation to the SLAM robot for an indoor exploration, a rectangle-oriented topological navigation function is presented based on the method mentioned in [9].

To apply the Navigation function, three types of spaces are considered: world space $\mathscr{W}$, free configuration space $\mathscr{F}$, and model space $\mathscr{M}$. Example of these worlds are shown in Fig. 1. World space $\mathscr{W}$ in Fig. 1(A) corresponds a real space where

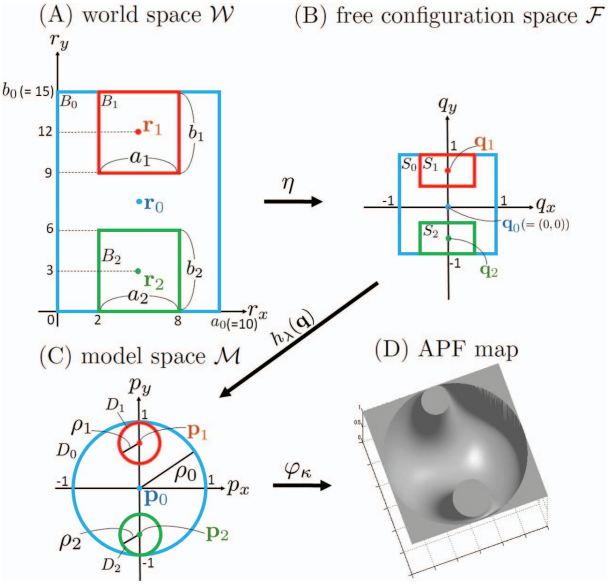

Fig. 1. Conceptual example of three types of spaces for Navigation function [13]

the robot moves. Rectangular box elements one described by $B_i = \{r_{xi} \;\; r_{yi} \;\; a_i \;\; b_i\}$, where $(r_{xi}, r_{yi}) =: \mathbf{r}_i$ is a rectangular center, a is the side length of the rectangle, and b is the length of the vertical side of the rectangle. Most outer space of $\mathscr{W}$ is expressed with $i = 0$. Boxes indexed by $i = 1 \ldots M$ are assigned to obstacles. Here B_0 corresponds to the outer outside of the $\mathscr{W}$ space. $\mathscr{F}$ which is shown in Fig. 1(B) is a space made by the most outer area B_0 of $\mathscr{W}$, and it was converted into a square area bounded by ± 1 . The box element in $\mathscr{W}$ corresponds to the star-shape element S_i in $\mathscr{F}$. The star-shape area elements are specified by $S_i = \{q_{xi} \;\; q_{yi} \;\; a'_i \;\; b'_i\} \;\; (i = 0 \ldots M)$, where $(q_{xi}, q_{yi}) = \mathbf{q}_i$ is center coordinates of the star-shape, a'_i and b'_i are length and the short vicinity, respectively. Model space $\mathscr{M}$ in Fig. 1(C) is a topological space mapped from $\mathscr{F}$ by the diffeomorphic mapping. All elements are expressed by disks. The disk area is specified by $D_i = \{p_{xi} \;\; p_{yi} \;\; \rho_i\} \;\; (i = 0 \ldots M)$, where $(p_{xi}, p_{yi}) =: \mathbf{p}$ is center coordinate values of the disk, and ρ_i is a radius of area. In this paper, the algorithm in the most necessary part from Fig. 1(C) to Fig. 1(D) of navigation function is briefly explained below.

A. Linear combination map of conversion scale $h_\lambda : \mathscr{F} \to \mathscr{M}$

It is not exclusive to overlap each obstacle S_i of the $\mathscr{F}$ simply. Therefore, the topology structure of $\mathscr{F}$ space

cannot be mapped onto $\mathscr{M}$. Therefore, a linear combination of each element is realized by analytic switch which makes neighborhood of each obstacle element available scope. This "linear combination of conversion scale" is defined as follows.

$$h_\lambda(\mathbf{q}) \triangleq s_d T_d(\mathbf{q}) + \sum_{i=0}^{M} s_i T_i(\mathbf{q}), \qquad (\in \mathbf{p} \ \text{ in } \ \mathscr{M}), \tag{9}$$

where each term of Eq. (9) is defined as

$$T_d(\mathbf{q}) \triangleq h_d(\mathbf{q}), \tag{10}$$

$$T_i(\mathbf{q}) \triangleq \nu_i \cdot [\mathbf{q} - \mathbf{q}_i] + \mathbf{p}_i, \tag{11}$$

$$\nu_i(\mathbf{q}) \triangleq [1 + \alpha_i(\mathbf{q})]^{\frac{1}{2}} \frac{\rho_i}{\| \mathbf{q} - \mathbf{q}_i \|}, \tag{12}$$

where h_d is the identity mapping and ν_i is the scaling factor, and α_i is the obstacle function for rectangle.

B. Navigation function

The value of APF is calculated by using navigation function for the point $\mathbf{p}$ on $\mathscr{M}$. Considering the range of obstacle function, navigation function φ_κ in this method, calculated by

$$\varphi_\kappa(\mathbf{p}) = \frac{\| \frac{\mathbf{p}-\mathbf{p}_d}{2} \|^2}{\left[\| \frac{\mathbf{p}-\mathbf{p}_d}{2} \|^{2\kappa} + \beta(\mathbf{p}) \right]^{1/\kappa}}, \tag{13}$$

where $\beta(\mathbf{p})$ is given in spherical obstacle function of the Euclidean sphere model version by following

$$\beta = \prod_{i=1}^{M} \beta_i(\mathbf{p}), \tag{14}$$

$$\beta_i(\mathbf{p}) \triangleq \| \mathbf{p} - \mathbf{p}_i \|^2 - \rho_i^2, \qquad i = 1, \cdots, M. \tag{15}$$

IV. Simulation

A. Simulation of environmental map generation which uses SLAM

The comb-shaped marker is set up on the wall, and whether SLAM can be done by extracting the marker as LM is confirmed. Whether the position of the wall, LM, and the robot was obtained from the quasi-data acquired with LRF was confirmed this time. The size of $\mathscr{W}$ is assumed H type space in 10×15[m]. Figure 2 is shown the position of the wall, LM, and the robot which calculates from the LRF data obtained by the simulation. In Fig. 2, blue line are a wall obtained from LRF data, and the part where the wall projects straight is a part of the comb-shaped marker. Moreover, a red line is an orbit where the robot was moved. This orbit is calculated from the LRF data and the position of the robot which is given the true value.

B. The moving object avoidance simulation which uses the Navigation function

Whether a safe distance is kept between the robot and the obstacle is verified when the robot is moved by using the Navigation function in a dynamic environment. The robot will be moving to the target position without colliding with the obstacle if there is a distance difference between the point mass robot and the obstacle. This text simulates whether the

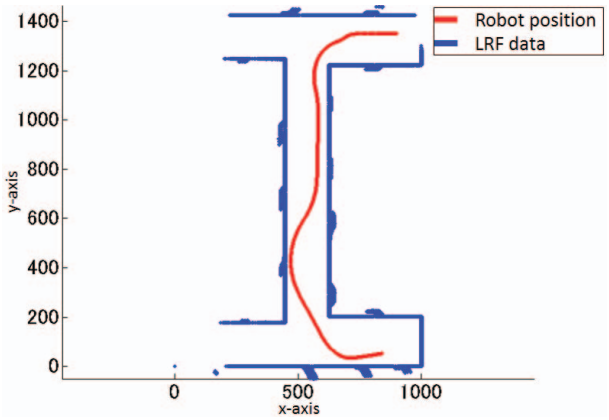

Fig. 2. Position of the robot and the wall and LM

point mass robot can be moved to the target position by avoiding the moving object by APF in $\mathscr{M}$. Size of work space $\mathscr{W}$ was assumed 14.25×10.66[m] and the center was assumed $(7.125, 5.33)$. This work space and two movement obstacles which are behaved different are mapped to $\mathscr{M}$. The 1st movement obstacle is assumed $[{}^A x(t), {}^A y(t)]$, the 2nd movement obstacle is assumed $[{}^B x(t), {}^B y(t)]$, and they are moved by the following expressions.

$$\begin{cases} {}^A x(t) = t, \\ {}^A y(t) = \frac{7.66}{49}(t-7)^2 + 3, \end{cases} \tag{16}$$

$$\begin{cases} {}^B x(t) = t, \\ {}^B y(t) = 3\sin(2t) + 5, \end{cases} \tag{17}$$

where $t \in [0, 10]$ is time. Equation (13) and (14) were designed because the subject of studies is children who locomote in the kindergarten. It was simulated at two cases which the start position and the goal position of the robot in the work space $\mathscr{W}$ were different. The 1st case was assumed the start position $S_1 = [1, 1]$ and the goal position $G_1 = [13, 9]$, and the 2nd case was assumed the start position $S_2 = [2, 9]$ and the goal position $G_2 = [7, 3]$. These are shown like the following Fig. 3. The amplitude and the frequency of the moving obstacle of Eq. (17) have been changed to confirm the robustness. Where the

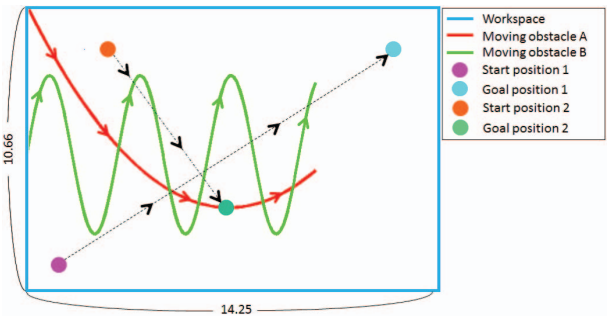

Fig. 3. Example of posture of the work space and the moving obstacles in $\mathscr{W}$

radius of the moving obstacles in $\mathscr{M}$ are assumed to be 0.03. The point mass robot avoids the moving obstacles, and the simulation result which was attained to the goal point is shown

in Fig. 4. The starting point and the goal point of the point mass robot are the 1st case shown Fig. 4(A), and are the 2nd case shown Fig. 4(B).

The distance difference between two moving obstacle and

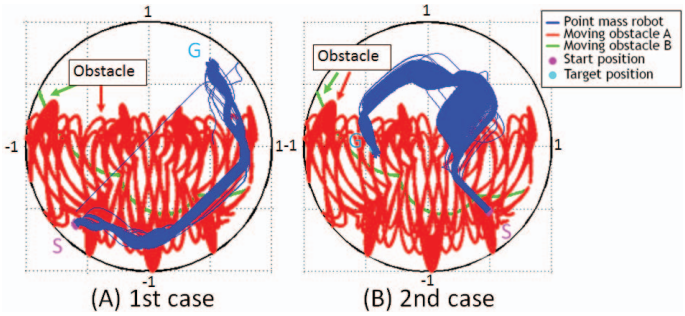

Fig. 4. Path of the point mass robot in $\mathscr{M}$

the point mass robots is shown in Fig. 5. The simulation of the 1st case is shown Fig. 5(A), and of the 2nd case is shown Fig. 5(B). In Fig. 5(A), It is understood that it is larger than the radius of the moving obstacle also even from the part where the distance difference is the smallest. In Fig. 5(B), the same thing of the robot and the movement object can be said. Therefore, the robot did not collide to any obstacles. Thus, the robot navigation was succeeded.

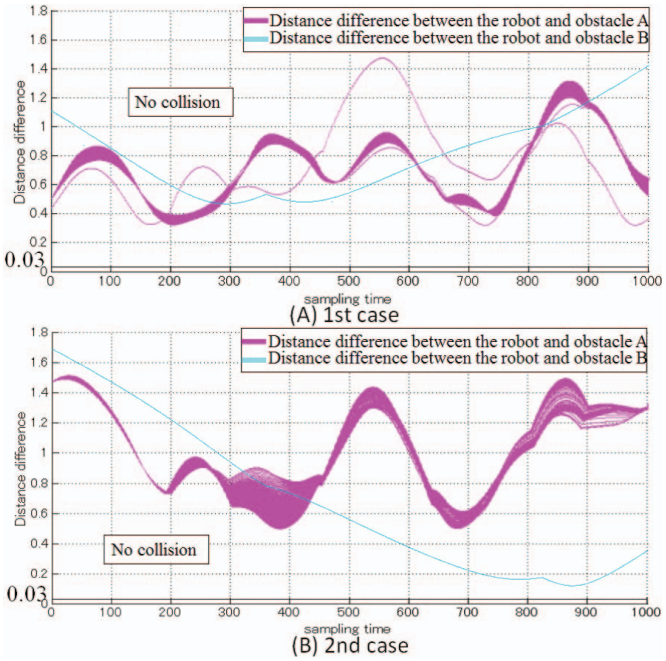

Fig. 5. Distance difference of point mass robot and each moving object

V. Conclusion

It aimed for the mass robots to use both SLAM and APF in a dynamic environment where the moving obstacles existed and to verify the movement possibility to a target position. Then, whether the position of the wall, LM, and the robot was able to be calculated from the data of LRF when SLAM was used was confirmed. Moreover, whether the mass robot be able to avoid the moving obstacles in a dynamic environment when the start position and the goal position of the point mass robot were changed and move to a target position were verified. As a result, the robot was able to be moved to the target position without colliding with the moving obstacles in the topology space. Even if the behavior of the moving obstacle was changed, the robot was able to avoid the moving obstacles. Thus, the robot navigation was succeeded.

As a view in the future, whether it is possible to move as SLAM and APF are combined by $\mathscr{W}$ and the robot evades the movement object is confirmed. Moreover, whether it is possible to move avoiding the moving obstacles with a real machine if this is possible will be verified.

References

[1] Survey results on the baby-related services market 2010, Yano Research Institute Ltd., 2010

[2] Nursery-kindergarten management support system, ANS Ltd.

[3] Children and child care support system, YPC

[4] S. Suzuki, Y. Mitsukura, H, Igarashi, H. Kobayashi, and F. Harashima, Activity Recognition for Children using Organizing Map, in Proc. of 21st IEEE International Symposium on Robot and Human Interactive Communication (RO-MAN2012), 2012

[5] C. Abrego and P. Shiakolas, Adding Obstacle Avoidance to a Robotic Platform for Human Robot Interaction, PErvasive Technologies Related to Assistive Environments, No. 58, 2013

[6] S. Hamasaki and Y. Tamura, A. Yamashita and H. Asama, Prediction of Human' s Movement for Collision Avoidance of Mobile Robot, International Conference on Robotics and Biomimetics, pp. 1633-1638, 2011

[7] L. Lee, Decentralized Motion Planning within an Artificial Potential Framework (APF) for Cooperative Payload Transport by Multi-Robot Collectives, Mechanical and Aerospace Engineering, 2004

[8] T. Nakamura and S. Suzuki, Kindergarten SLAM utilizing Laser range sensor and retro-reflective markers, Industrial Electronics Society, pp. 8300-8305, 2013

[9] E. Rimon and D. Koditschek, Exact Robot Navigation Using Artificial Potential Functions, IEEE Transactions on Robotics and Automation, Vol. 8, No. 5, pp. 501-518, 1992